arXiv:1605.09467v1 [astro-ph.SR] 31 May 2016

The diamagnetic phase transition of dense electron gas: astrophysical applications

Zhaojun Wang[1], Guoliang Lü[1], Chunhua Zhu[1], Baoshan Wu[1]
xjdxwzj@sohu.com, guolianglv@gmail.com

ABSTRACT

Neutron stars are ideal astrophysical laboratories for testing theories of the de Haas-van Alphen (dHvA) effect and diamagnetic phase transition which is associated with magnetic domain formation. The "magnetic interaction" between delocalized magnetic moments of electrons (the Shoenberg effect), can result in an effect of the diamagnetic phase transition into domains of alternating magnetization (Condon's domains). Associated with the domain formation are prominent magnetic field oscillation and anisotropic magnetic stress which may be large enough to fracture the crust of magnetar with a super-strong field. Even if the fracture is impossible as in "low-field" magnetar, the depinning phase transition of domain wall motion driven by low field rate (mainly due to the Hall effect) in the randomly perturbed crust can result in a catastrophically variation of magnetic field. This intermittent motion, similar to the avalanche process, makes the Hall effect be dissipative. These qualitative consequences about magnetized electron gas are consistent with observations of magnetar emission, and especially the threshold critical dynamics of driven domain wall can partially overcome the difficulties of "low-field" magnetar bursts and the heating mechanism of transient, or "outbursting" magnetar.

Subject headings: star:neutron—magnetic fields—Pulsar: general

1. Introduction

Degenerate Fermi electron gases occur in a huge variety of systems for a wide range of density from non-relativistic metals to relativistic neutron stars. Regardless of the particular substance, there should appear to be quite similar over all magnetized systems in an applied or external magnetic field. During a helical motion around the magnetic field, electron energy is quantized into discrete Landau levels. If the successive Landau level interval is higher than thermal energy of the system, $\hbar\omega_c \geq k_B T$, electron gas can exhibit the nonlinear de Haas-van Alphen (dHvA) effect. Here, $\hbar$ and k_B respectively are the Planck and Boltzmann constants, ω_c is the cyclotron frequency. Whenever the Fermi energy approaches to the Landau level, the magnetization oscillates rapidly with the field. The oscillation is sinusoidal with a fundamental frequency determined by an extremal area of the cross-section of the Fermi surface which is normal to the applied magnetic field (Lifshits & Kosevich 1956).

Using the impulsive field method, Shoenberg (Shoenberg 1962) found an additional high amplitude in the second harmonic of the dHvA oscillation, and proposed the concept of "magnetic interaction" among the conduction electrons. This interaction stems from the overlap of helical orbits of electrons. For this reason, an electron actually feels the magnetic induction (or magnetic flux density) B instead of the magnetic field H. Usually, the difference between B and H is $4\pi M$ and small, where M is the oscillating part of magnetization (we use Gaussian units in this paper). However, if the magnetic interaction is large enough so that the amplitude of magnetization oscillation can be comparable with their period, the interaction may lead to a phase transition. This transition belongs to a particular instability of electron gas, the so-

[1]School of Physical Science and Technology, Xinjiang University, Urumqi, 830046, China

called diamagnetic phase transition (Privorotskii 1976). More accurately, when the differential magnetic susceptibility of electron gas, $\chi_{\rm m} = \partial M/\partial B$, is greater than $1/4\pi$, $\partial B/\partial H$ is negative and is not physical. The stable state will have a spatial inhomogeneous structure of magnetic field with domains (i.e., Condon's domains (Condon 1966)) in which the magnetic induction and the magnetization can take one of two different values. There is a transitional layer called domain wall (DW) between neighboring domains with variation of magnetization. These magnetic domains have been observed in some metals such as silver, beryllium, etc. (Condon 1966; Solt et al. 1996, 1999, 2000; Solt & Egorov 2002). More extensive review of theoretical and experimental progress about the diamagnetic transition in metals can be found in Gordon, Egorov, etc. (Gordon et al. 2003; Egorov 2010). Magnetizing process under a changing applied field would accompany DW displacement. However, the motion is damped by the inhomogeneities (e.g., crystalline imperfections) of the medium from which typical dynamical critical phenomena (called depinning transitions) can take place. All the essential elements of the depinning motion of DW, as discovered in experiments of the Barkhausen (BK) effect, are the avalanche-like statistical properties of the magnetization noise: distribution of size and duration of the avalanches, etc. (Alessandro et al. 1990; Narayan 1996; Zapperi et al. 1998).

Although all the theoretical and experimental conclusions as stated above are limited to non-relativistic electron gases, we can extend these results to neutron stars and their different subclasses, such as magnetar especially. Magnetars, including Anomalous X-ray Pulsars (AXPs) and Soft Gamma Repeaters (SGRs), are characterized by their inferred dipolar magnetic field which is in the range of $5.9 \times 10^{13} - 1.8 \times 10^{15}$ G, and their long spin periods $5.2 - 11.8$ s. The most significant feature is the emission of X-ray or γ-ray bursts and occasionally giant flares (with duration of $0.1-10$ s, flux intensity of $10^{34}-10^{47}$ ergs s^{-1} at the peak) (Woods & Thompson 2006; Mereghetti 2008; Turolla et al. 2015). There is a consensus on the energy source of the persistent and bursts emission powered by magnetic energy. Until now, however, the emission mechanism remains an open question. In a framework of starquake model, the evolution of the field imposes stress on solid crust of neutron star, which is deformed elastically until catastrophical rupture (Thompson & Duncan 1995a). However, whether the elastic energy storing in crust could power the giant flares and the "low-field" magnetars could been ruptured are still under debate (Thompson & Duncan 1995a; Rea et al. 2010). In the last few years, almost all new observed magnetars are transient magnetars marked by the "outbursting" (Ibrahim et al. 2004; Turolla et al. 2015). This outbursting mechanism has been explained as due to heat deposition into the star surface, and then the limited region cools and shrinks (Pons & Rea 2012). Until now, the unambiguously heating mechanism has not been identified.

The starquake model is strongly motivated by a similarity of statistical distribution of SGR bursts and earthquakes (Cheng et al. 1996; GöğüŞ et al. 1999). Such distribution belongs to self-organized criticality (Chen et al. 1991) in general. However, the universal statistical aspects of SOC do not suggest that magnetar bursts are necessarily from the crustquakes. Similar statistical distributions have been found in solar flares (Lu et al. 1993) and in the BK effect of magnetic materials (Durin & Zapperi 2004). Inside a neutron star, the magnetic field configuration and matter distribution under some suitable conditions can satisfy the following three necessary conditions of the BK effect, i.e., the existences of: (1) magnetic domains; (2) disordered defects; and (3) a slowly changing magnetic field. There is no serious drawback about the domain formation of a neutron star as having been proved in (Blandford & Hernquist 1982; Suh & Mathews 2010; Wang et al. 2013) etc. **Suh & Mathews (2010) considered the magnetization and susceptibility of magnetar matter for three different equations of state. They concluded that the magnetic susceptibility can lead to the formation of magnetic domains and a possible observable consequence of the SGRs bursts. However, it has not yet been demonstrated how the magnetic domains actually evolve and the disordered effect of the crust matter.** Recent calculations about disordering defects (impurities, dislocations, grain boundaries, etc.) in the crust of a neutron star give a large impurity factor $Q \geq 10$ (Jones 2001; Horowitz & Kadau

2009) implying the presence of a very strong magnetic hysteresis. At late times of the field evolution of a neutron star (especially magnetar), the Hall effect of short evolution timescale will dominate Ohmic decay (Cumming et al. 2004). In spite of non-dissipation, the Hall effect can release magnetic energy through a turbulent Hall cascade (Goldreich & Reisenegger 1992) which is only or partially associated with the persistent emission of the magnetar. However, after considering the damp and jerky motion of DW, the Hall effect looked as if a continuous power provision source can temporarily store the energy, which contributes a series of sudden, incomplete releases of the accumulated energy. This behaves like in a relaxation system of Palmer (Palmer 1999). This mechanism does not require absolutely crumbling of the crust and can be regarded as a heating mechanism of the transient magnetar.

In this paper we consider particularly a degenerate extreme-relativistic electron gas in the background of a crystal lattice under a strong magnetic field. Except the magnetic interaction, we neglect other complicated interactions of electrons with each other or with the lattice viration. Under these conditions, the extension of the dHvA effect and the diamagnetic phase transition to a relativistic electron gas is simply the replacement of the cyclotron mass by the relativistic mass. Using a very simple domain configuration, we calculate the sizes of the domain thickness and the surface tension of the DW in its static state. Finally, we propose possible observational effects of the diamagnetic transition, e.g., the magnetostriction effect and the BK effect of dense matter.

The paper is organized as follows: In §2, we review the general theory of the dHvA effect and generalize the Lifshitz-Kosevich-Shoenberg theory to relativistic electron gas of a neutron star. In §3, we give the conditions of the diamagnetic phase transition and the corresponding phase diagram in a relativistic electron gas with a spherical Fermi surface. In §4, we examine the static structure of domains and calculate the sizes of domain thickness and the surface tension of DW. In §5, we discuss the possible observational applications to magnetars. Finally, Section §6 is devoted to our main conclusions and discussions.

2. General theory of de Haas-van Alphen effect and application to dense matter

For the completeness, we first briefly review the Lifshitz-Kosevich-Shoenberg theory of magnetic oscillation in metals. It is generalized to the case of a dense matter (such as neutron star) with a similar Coulomb crystal lattice structure. A detailed presentation about magnetic oscillation in metals is given by Shoenberg in (Shoenberg 1984). For generalization and application to a dense matter, we consider a typical neutron star crust consisting of a neutron rich lattice in which the given nucleus (with the nuclear charge Z) is present. Most of this crust is in a radial shell of thickness about 10^5 cm and total baryon density, ρ, in the range $10^6 - 10^{14}$ g.cm^{-3}.

2.1. The theory of de Haas-van Alphen effect

A realistic system of conducting electrons in metal should be treated as a Fermi liquid having complicated many-body interactions of electrons (with e.g., each other, phonons or magnons). However, for a magnetic oscillation theory about a system of approximately independent quasi-particles, the behavior is determined by the dispersion relation, $\varepsilon(\vec{k})$, an arbitrary dependence of energy on wave vector $\vec{k}$, which is specified by the periodic crystal potential. Acted on by a magnetic field, the classical trajectory of a quasi-electron will be helical with a cyclotron frequency, $\omega_{\rm c}$, given by

$$\omega_{\rm c} = \frac{2\pi eB}{c\hbar^2} \Big/ \left(\frac{\partial s}{\partial \varepsilon}\right)_{\kappa_z} = \frac{eB}{mc} \ . \qquad (1)$$

where the cyclotron mass is defined as $m = (\hbar^2/2\pi)(\partial s/\partial\varepsilon)_{\kappa_z}$, $-e$ is the electronic charge, c is the velocity of light in vacuum, κ_z is the component of the wave vector along the magnetic field (in the z direction), s is the area of the cross section of the constant energy surface at arbitrary κ_z in the wave vector space. Actually, the area s is quantized and satisfies the famous Onsager relation

$$s\left(\varepsilon, \kappa_z\right) = \left(r + \frac{1}{2}\right) \frac{2\pi eB}{c\hbar} \qquad (r = 0, 1, \cdots) \ . \qquad (2)$$

At the ground state of an independent electron gas, all occupations take place within the Fermi

surface (FS). As the field increases, the length of κ_z with the largest area, which will partially inside the FS, will shrink and vanish infinitely rapidly when the area s equals the extremal area A of the cross-section of the FS at κ_z. Such a special occupation happens periodically with a fundamental frequency F

$$F = \frac{c\hbar}{2\pi e}A. \tag{3}$$

For each of such occupations, the energy and magnetization experience oscillations as the field varies. The oscillatory functions are sinusoidal series with a fundamental frequency that can be described by the extremal areas A as Eq.(3). The absolute oscillation amplitude is proportional to $|A''|^{-1/2}$ where $A'' = (\partial^2 s/\partial\kappa^2)_{\kappa=0}$. Some corrections from finite temperature T, finite electron relaxation time τ due to scattering, and electron spin can be introduced independently as phase smearing that leads simply to a multiplication factor for every harmonic term. If the separation of successive Landau levels is larger than its thermal and scatting energies, that is, $\hbar\omega_c > k_B T$ and $\hbar\omega_c > 2\pi\hbar/\tau$, the oscillatory magnetization per unit volume in the direction of the applying magnetic field is given by (Shoenberg 1984)

$$\begin{aligned} M = \; & -(\tfrac{e}{c\hbar})^{3/2}\tfrac{2Fk_BT}{(2\pi B|A''|)^{1/2}} \\ & \textstyle\sum_{p=1}^{\infty}\tfrac{\exp(-2\pi^2 p\omega_e/\omega_c)\cos[p\pi(\Delta\varepsilon_s/\hbar\omega_c)]}{p^{1/2}\sinh(2\pi^2 pk_BT/\hbar\omega_c)} \\ & \times\sin[2\pi p(\tfrac{F}{B}-\tfrac{1}{2})\pm\tfrac{\pi}{4}]\ , \end{aligned} \tag{4}$$

where "+" or "-" corresponds to the case of the minimum or maximum extreme section respectively, $\omega_e = 2\pi/\tau$ is the scatting frequency, $\triangle\varepsilon_s/2$ is the energy lifting due to the spin degeneracy. The Lifshitz-Kosevich-Shoenberg formula of magnetization given above is principally determined by the configuration of the constant energy surface. It can be generalized to a relativistic electron gas in a neutron star.

2.2. Application of de Haas-van Alphen effect to dense matter

Neutron star is one of the degenerate stars with electron and neutron degenerations. Inside the deep crust of a neutron star, the electron gas can be regarded as completely degenerate and extremely relativistic. The Fermi energy ψ_0 in the absence of a magnetic field is given by

$$\psi_0 = (3\pi^2)^{1/3}c\hbar n_e^{1/3} \approx 51\rho_{12}^{1/3}Y_e^{1/3}\ \text{MeV}, \tag{5}$$

where n_e is the number density of the electron gas and ρ_{12} (scaling as 10^{12} g cm^{-3}) is the mass density of the crust, Y_e is the number fraction of electrons. Recent calculations of the Fermi energy can be found in Li et al. (2016). Eq.(5) indicates that the Fermi energy is by far larger than the rest-mass energy of the electrons, $\mu \equiv m_e c^2 \approx 0.5$MeV (where m_e is the rest mass of electron), and much larger than the thermal kinetic energy $k_B T$ ($k_B T < 1$ KeV (Pons et al. 2007)). Considering the lattice energy per electrons (Coldwell-Horsfall & Maradudin 1960), $\varepsilon_l \approx 3.4\times10^{-3}Z^{2/3}\psi_0$, which is by far smaller than the Fermi energy, we can treat the electron system more accurately as an ideal gas.

A relativistic electron in an applied magnetic field is quantized with the dispersion relation (Johnson & Lippmann 1949)

$$\varepsilon^2 = c^2\hbar^2\kappa_z^2 + \mu^2 + \frac{c^2\hbar^2}{\pi}s = m^2c^4\ , \tag{6}$$

where m is the relativistic mass of the electron, the quantized area of cross section s takes its values as those given in Eq.(2). From this dispersion relation we find that the cyclotron frequency ω_c is given

$$\omega_c = \frac{2\pi eB}{c\hbar^2}\Big/\left(\frac{\partial s}{\partial\varepsilon}\right)_{\kappa_z} = \frac{eB}{mc}\ . \tag{7}$$

This result indicates that the electron cyclotron mass is equal to it's relativistic mass.

The maximum area of the cross section A can be obtained from Eq.(6) with $\kappa_z = 0$ and $\varepsilon = \psi$ (ψ is the chemical potential of the electron gas in an applying field).

$$A = \frac{\pi}{c^2\hbar^2}(\psi^2 - \mu^2) \approx \frac{\pi}{c^2\hbar^2}\psi^2\ , \tag{8}$$

where we have supposed $\psi \gg \mu$ for the case of a neutron star. The fundamental frequency F of Eq.(3) relates to B via

$$\frac{F}{B} \approx \frac{1}{2}\left(\frac{\psi}{\mu}\right)^2\frac{B_Q}{B}\ , \tag{9}$$

where $B_Q = 4.41\times10^{13}$ G is the quantum magnetic field of the electron. The value of $|A''| = 2\pi$ can be easily obtained from Eq.(6).

The energy separation between successive r at a fixed κ_z is given by (when the quantum number r is by far larger than 1)

$$(\triangle\varepsilon)_{\triangle r=1}=\left(\frac{\partial\varepsilon}{\partial s}\right)_{\kappa_z}(\triangle s)_{\triangle r=1}=\hbar\omega_{\rm c}\ , \quad (10)$$

which is formally similar to the energy spacing in a no-relativistic case except the rest mass now being replaced by the relativistic one at the Fermi surface. Applying magnetic field makes the spin degeneracy of the energy levels lifted to,

$$\varepsilon=[c^2\hbar^2\kappa_z^2+\mu^2+(2r+1+s')\mu\epsilon_{\rm c0}]^{1/2}\ , \quad (11)$$

where $s'=\pm1$ and $r=0,1,\cdots$, are the spin and Landau quantum numbers of electron respectively. $\epsilon_{\rm c0}=(eB/m_{\rm e}c)$ is the cyclotron energy of an electron in the non-relativistic. Near the FS, the energy splitting due to electron spin is small and can be expanded in Taylor series. To the first order, the energy spilling is

$$\varepsilon\approx\psi\pm\frac{1}{2}\triangle\varepsilon\approx\psi\pm\frac{1}{2}\hbar\omega_{\rm c}\ , \quad (12)$$

where "-" or "+" corresponds to the spin-up and spin-down respectively. The reduction factor of $\cos(p\pi\triangle\varepsilon/\hbar\omega_{\rm c})$ in Eq.(4) due to the spin is equal to $(-1)^{\rm p}$.

Keeping only the lowest-order term, the final form of Eq.(4) is given by

$$4\pi bM=a(T,T_{\rm D},H_0)\sin[b(h+4\pi M)]\ , \quad (13)$$

where $H_0=B_0$ is the magnetic field of the center of an oscillation cycle, $h=H-H_0$ denotes the deviation of the magnetic field H from H_0 (supposing $h\ll H_0$), $b=2\pi F/B_0^2$. In Eq.(13), we have neglected the constant phase. The reduced amplitude of magnetization due to thermal temperature, Dingle temperature $T_{\rm D}$ (or the relaxation time of the electron scatting, $\tau=2\pi\hbar/kT_{\rm D}$) is given by

$$a(T,T_{\rm D},B_0)=a_0(B_0)\frac{\lambda T}{\sinh(\lambda T)}\exp(-\lambda T_{\rm D})\ , \quad (14)$$

$$a_0(B_0)=\frac{\alpha}{\pi}\left(\frac{\psi}{\mu}\right)^3\left(\frac{B_{\rm Q}}{B_0}\right)^{3/2}\ , \quad (15)$$

where α is the fine structure constant, $\lambda=2\pi^2k_{\rm B}/\hbar\omega_{\rm c0}$ and $\omega_{\rm c0}$ takes the value of Eq.(7) with $B=B_0$. This result is formally similar to the one given in metals (Gordon et al. 1999), and also similar to the result presented in (Wang et al. 2013), in which the temperature and scatting effects were neglected.

Under a strongly quantizing magnetic field which can be prevailed in the magnetar interior or the most out-crust, only a few Landau levels are occupied. Then, the above theory and calculations about the electron gas magnetization cannot be applied. In this case, matter behavior and the equation of state at the thermodynamical equilibrium or the nonequilibrium β-process have been studied in Lai & Shapiro (1991); Chamel et al. (2012); Basilico et al. (2015); Wang et al. (2014), etc. In Wang et al. (2014), we have analytically calculated the magnetization of the electron gas acted with strongly quantizing magnetic field. The magnetization exhibits also the similar oscillatory behavior as that described by Eq.(4).

It should be noted that the Lifshitz-Kosevich-Shoenberg theory to a neutron star is applicable only in simple models of independent electrons. The finite temperature effect is treated as only blurring out slightly the boundary of the occupation and the un-occupation, and within a finite relaxation time only blurring out the sharpness of quantized states. The general magnetization theory of an electron system should consider the many-body interactions (with each other or with phonons or magnons). A quite general result of the interactions is the modification of the dispersion relation $\varepsilon(\vec{k})$ of the independent particle model. Firstly, the independent particle energy is shifted to a dynamical quasi-particle energy with an additional term , $\varepsilon=\varepsilon(\vec{k})+\triangle(\varepsilon-\psi)$. Secondly, the energy is broadened according to the Lorentzian fashion characterized by a parameter $\Gamma(\varepsilon-\psi)$, where ψ is chemical potential of the electron system. These modifications can be obtained by quoting a basic concept of the self energy which is a complex quantity denoted by $\sum(\varepsilon-\psi)=\triangle(\varepsilon-\psi)-i\Gamma(\varepsilon-\psi)$. As Shoenberg had showed (Shoenberg 1984), the Lifshitz-Kosevich-Shoenberg formula of an independent electron system remains valid, but the parameters have to be modified appropriately. The basic theory about the effect of many-body interactions is beyond the scope of this paper (for detailed discussions of electron-electron and electron-phonon interac-

tions readers are referred to Luttinger (1960) and Engelsberg & Simpson (1970)).

3. The diamagnetic phase transition of relativistic electrons inside a neutron star

Eq.(13) is the correct form of the Lifshitz-Kosevich formula after Shoenberg's magnetic interaction is taken into account. In its derivation, we have implicitly assumed that the magnetization is a function of the magnetic induction, i.e., $M = M(B)$. This suggests that the magnetization depends also on the ordering of the orbital magnetic moments of electrons. Usually, the difference between B and H is very small. If the amplitude of the magnetization oscillation is comparable with their period, however, the interaction can lead to the diamagnetic phase transition. In this case, the self-consistent solution of Eq.(13) about the magnetization is multiple-valued. In fact, as discussed in Condon (1966), the material will separate into two phases with parallel and anti-parallel magnetizations. This transition is different from the ferromagnetic transition. In the former the magnetic ordering comes from the classical magnetic interaction, while in the latter it is from the quantum exchange interaction. The diamagnetic phase occurs in each cycle of the dHvA oscillations whenever the reduced amplitude of the oscillations is equal to 1, $a(T_{\rm d}, T_{\rm D}, B_0) = 1$, where $T = T_{\rm d}$ is the critical temperature.

One of the necessary conditions of the diamagnetic phase transition is $a_0(B_0) > 1$ given in Eq.(15). According to ψ_0 of Eq.(1), we can approximately take $\psi \approx \psi_0$ in spite of that the chemical potential of an ideal electron gas slowly declines with the increase of the magnetic field (Ingraham & Wilkes 1987). From Eq.(15), the condition is

$$B_0 < \left(\frac{\alpha}{\pi}\right)^{2/3} \left(\frac{\psi_0}{\mu}\right)^2 B_{\rm Q} \ . \qquad (16)$$

If we take a value of $\psi_0 \sim 25$ MeV inside the deep crust, Eq.(16) becomes $B_0 < 44 B_{\rm Q}$ (the rest energy of an electron is about $\mu \sim 0.5$ MeV). Almost all of the normal neutron stars including magnetars satisfy this condition. While some SGRs with a magnetic field near $100 B_{\rm Q}$ (e.g. SGR 0526-66, SGR 1806-20, SGR 1900+14), only the diamagnetic phase transitions occur in the liquid core or/and inner crust as sketched in Fig.1.

The condition of a large Landau quantum number requires $\psi_0 \gg \hbar\omega_{\rm c}$. From the definition of $\omega_{\rm c}$ in Eq.(7), this condition is satisfied as long as

$$\psi_0 \gg \mu \left(\frac{B_0}{B_{\rm Q}}\right)^{1/2} \ . \qquad (17)$$

Except for some very particular cases of low Landau quantum number occupations, the Lifshitz-Kosevich-Shoenberg theory is adequate. Actually, Shoenberg (1984) suggested the largest quantum number $r_{\rm max} > 2$. If $r_{\rm max} \leq 2$, the diamagnetic phase does not really occur in spite of the similar oscillation property of Eq.(4) (Wang et al. 2014).

Chamel et al. (2012) has given the out crust structure and composition of a neutron star based on experimental data of atomic mass and complemented with theoretical prediction of the Hartree-Fock-Bogoliubov method (Goriely et al. 2010). Their results only included the effect of the Landau quantum of the electron gas in a strong magnetic field. However, the analysis of Basilico et al. (2015) accounted for the influence of the field on the nuclear binding energy and showed that the binding energy does not increase by more than 10%. The predicted composition in the two cases is similar, and the main difference is in the most outer crust (Basilico et al. 2015). Using the results of the outer crust structure and combining those of Chamel et al. (2012) at zero-temperature, the possible phase transition regions ($a_0 > 1$) are indicated in Fig.1.

The effects of finite temperature T, finite electron relaxation time τ due to the impurity scattering, had been introduced independently as phase smearing that lead to a multiplication factor $\lambda T/\sinh(\lambda T)$ and $\exp(-\lambda T_{\rm D})$ in Eq.(14) respectively. However, as shown in standard textbooks Landau & Lifshitz (1969), there are other necessary conditions of the magnetic oscillation restraining the temperature and electron relaxation. If the separation of successive Landau levels near the Fermi surface is not larger than the thermal kinetic and scatting energies, $\hbar\omega_{\rm c} < kT$ and $\hbar\omega_{\rm c} < kT_{\rm D}$, the diamagnetic phase does not occur. The Dingle temperature from impurity

(Itoh & Kohyama 1993) is

$$T_{\rm D} \approx 3.3 \times 10^6 \Lambda_{\rm eQ} (\frac{\epsilon}{100})(\frac{Z}{40})^{-1}(\frac{Q}{10})\ {\rm K}, \quad (18)$$

where $\Lambda_{\rm eQ}$ is the Coulomb logarithm of order unity, $\epsilon = \psi/\mu$, and Q is the impurity factor which is defined as the mean square charge deviation $\langle(\triangle Z)^2\rangle$. Here we have scaled the impurity Q by a large value $Q \sim 10$ (Jones 2001).

Combining all these necessary conditions given above with the critical condition of $a(T_{\rm d}, T_{\rm D}, B_0) = 1$, the phase transition curve can be determined from the following equations

$$T_{\rm d} = 0 \quad (\hbar\omega_{\rm c} \le k_{\rm B} T_{\rm D})\ , \quad (19)$$

$$T_{\rm d} = \hbar\omega_{\rm c}/k_{\rm B} \quad (k_{\rm B} T_{\rm D} < \hbar\omega_{\rm c} \le k_{\rm B} T_{\rm d})\ , \quad (20)$$

$$a_0 \frac{\lambda T_{\rm d}}{\sinh[\lambda T_{\rm d}]} \exp[-\lambda T_{\rm D}] = 1 \quad (\hbar\omega_{\rm c} > k_{\rm B} T_{\rm d}). \quad (21)$$

The range of the temperature of the phase transition in the outer crust of a neutron star with different magnetic fields are showed in Fig.2. The regions between the phase transition curves and the abscissa axis indicate the possibility of the diamagnetic phase transition. Figs.3 and 4 are the phase diagrams which show the phase-transition temperature as a function of the magnetic field for different matter densities. The value of the Fermi energy in Fig.3 is taken to be 25 MeV for strontium inside the deep outer crust, while in Fig.4 it is 2.5 MeV for iron envelope. The Dingle temperature, as a parameter in Figs.3 and 4, is taken as $Q = 10, 100$ in Eq.(18). The results indicate that the effect of the Dingle temperature is not obvious in the circumstance considered.

Taking Eq.(13) at $h = 0$ and expanding the right-hand side to the third order on M, we obtain an equation of order parameter, i.e., the magnetization in the Condon domains (Gordon et al. 1999).

$$\frac{M_{\rm s}}{B_0} = \pm 5 \times 10^{-5} \sqrt{\frac{3(a-1)}{2a}} \left(\frac{\epsilon}{100}\right)^{-2} \frac{B_0}{B_{\rm Q}}. \quad (22)$$

Eq.(22) indicates that the order parameter approaches to zero when the reduced amplitude $a(T, B_0, T_{\rm D})$ tends to 1. Near the critical point,

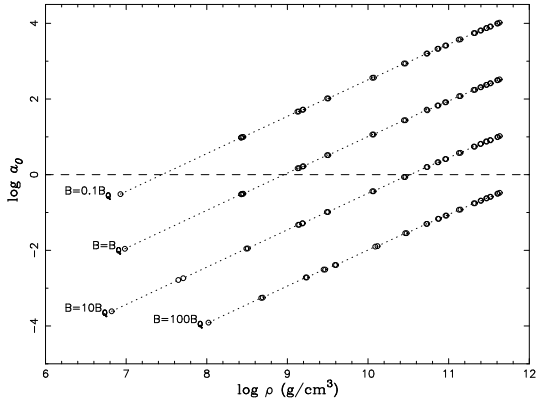

Fig. 1.— The largest amplitude of the dHvA oscillation a_0 in Eq.(15) versus neutron star densities inside the outer crust below neutron drip. The circles refer to numerical calculations of Chamel et al. (2012) for various compositions with different magnetic field ($B = 0.1B_{\rm Q}, B_{\rm Q}, 10B_{\rm Q}, 100B_{\rm Q}$). Long-dashed line ($a_0 = 1$) divide no (below line) and possible (above line) phase transition regions.

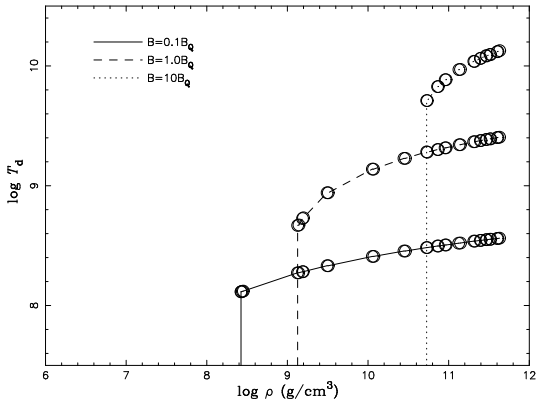

Fig. 2.— Phase diagrams for the diamagnetic phase transition in the outer crust. The phase-transition temperature is a function of matter densities, and the magnetic field and Dingle temperature ($Q = 10$) are choosen according to Eqs.19-21. The circles refer to the numerical calculations of Chamel et al. (2012) for various compositions with different magnetic fields.

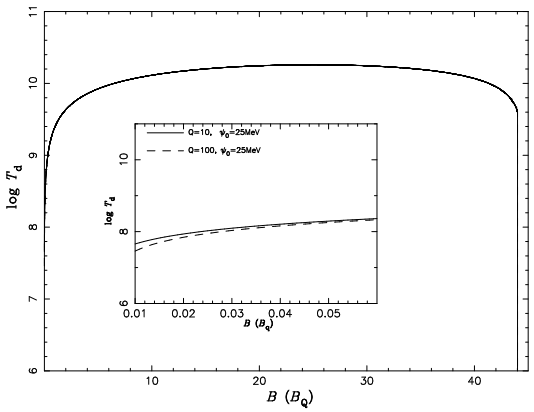

Fig. 3.— Phase diagrams for the diamagnetic phase transition versus the magnetic field in the deep outer crust ($\psi_0 = 25$ MeV). The Dingle temperature $Q = 10$ (solid line) or $Q = 100$ (dashed line) is taken as a parameter. The insert shows a distinguishable region for different Dingle temperatures.

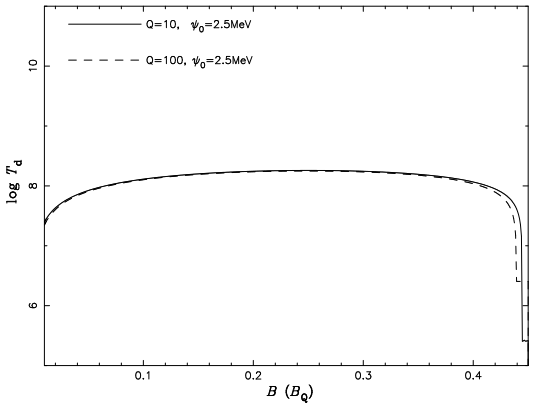

Fig. 4.— Phase diagrams for the diamagnetic phase transition versus the magnetic field in the deep outer crust ($\psi_0 = 2.5$ MeV). The Dingle temperature $Q = 10$ (solid line) or $Q = 100$ (dashed line) is taken as a parameter.

the order parameter is proportional to $(T_{\rm d} - T)^{1/2}$, showing the general characteristics of a continuous phase transition. "This fact is in agreement with the long-range character of magnetic interactions in the cooperative system of orbital magnetic moments of the electron gas" (Gordon et al. 1999). Far from the critical point, the fraction of the saturation magnetization, $M_{\rm s}/B_0$, is proportional to the central magnetic field at a fixed Fermi energy. Near the deepest outer crust, for example, $\epsilon \approx 50$ for $B_* = 0.1$ and $B_* = 100$ in table-4 and table-3. The fractions are approximately of 2.4×10^{-5} and 2.4×10^{-2}, respectively, indicating the potential importance of magnetizing in magnetars.

4. The Condon domain structure inside neutron star

The diamagnetic phase occurs in each cycle of the dHvA oscillation with a period determined by the magnetic field and Fermi energy of the electron gas. In the interior of the solid crust of a neutron star, both magnetic field and Fermi energy change on the depth from the crust surface. Thus, the possible phase transition regions are arranged in layers. In the layer structure, domain arrangement with alternate magnetization is energetically favorable by reducing the demagnetization energy as discussed by Condon (Condon 1966). Moreover, decreasing the domain width (meaning, increasing the number of domains) can reduce further the magnetostatic energy because of the rapidly falling off of the free magnetic poles. However, this is not favorable due to the increase of the magnetostatic energy of DWs. Minimizing the sum of these two contributions leads to an optimum domain size. Approximate calculations of the size of the simplest domain structure will be given below. For every domain layer of a neutron star, we first calculate the thickness and surface tension of DW.

4.1. The thickness and surface tension of DW

We start with the assumption that the wall thickness is of order of $d_{\rm c}$, the cyclotron diameter. Because of the inhomogeneous magnetization in this thickness, there is an additional free energy term in the thermodynamic potential density. The additional term is proportional to $(d\hat{m}/dx)^2$

where $\hat{m} = 4\pi bM$ is the dimensionless magnetization. Correspondingly, the thermodynamic potential density takes the form (Privorotskii 1976)

$$\Omega = \frac{1}{4\pi b^2}\left[a\cos(bh+\hat{m}) + \frac{1}{2}\hat{m}^2 + \frac{1}{2}K\left(\frac{d\hat{m}}{dx}\right)^2\right], \quad (23)$$

where K is the positive coefficient of the inhomogeneous term which is proportional to d_c^2. The dynamics of magnetizing in a non-zero external magnetic field is described by the Landau-Khalatnikov equation, $\partial M/\partial t = -\Gamma\delta\Omega/\delta M$, where Γ is the dynamic coefficient. For the potential density given by Eq.(23), we find,

$$\frac{\partial\hat{m}}{\partial t} = -4\pi a\Gamma\left[-\sin(bh+\hat{m}) + \frac{\hat{m}}{a} - \frac{K}{a}\frac{\partial^2\hat{m}}{\partial x^2}\right]. \quad (24)$$

This equation is ascribed to the nonlinear reaction diffusion equations. The static form of Eq.(24) has a kink solution. The thickness of a static DW is defined as $D = 2M_s/(\frac{dM}{dx}|_{x=0})$ which can be estimated as that given in Bakaleinikov & Gordon (2012). There are two limiting cases of a, one is that a is greater than and close to 1, and the other is that $a \gg 1$. For the first case, the thickness is given by

$$D = 6.7\times10^{-8}\frac{1}{\sqrt{a-1}}\left(\frac{\epsilon}{100}\right)\left(\frac{B_0}{B_{\rm Q}}\right)^{-1}\ {\rm cm}, \quad (25)$$

and for the second case it is

$$D = 7.4\times10^{-8}\left[1+\left(\frac{\pi^2}{8}-1\right)/a\right] \times \left(\frac{\epsilon}{100}\right)\left(\frac{B_0}{B_{\rm Q}}\right)^{-1}\ {\rm cm}, \quad (26)$$

where we have taken $K = d_c^2/4$. In the deep crust of a neutron star, the reduced effect of the oscillation magnitude due to temperature and scatting is neglected and $a \gg 1$. From Eq.(26), the thickness is the order of $D_0 \approx 0.5\pi d_{\rm c},$. This is indeed true, as the DW is order of the electron cyclotron diameter.

The surface tension σ of the DW, defined as $\sigma = \frac{1}{2}K\int_{-M_{\rm S}}^{M_{\rm S}}\frac{dM}{dx}dx$, can be calculated from the kink solution of the static equation of Eq.(24). As a function of deviation from the transition critical point $a-1$, the tension is

$$\sigma = 4.8\times10^{22}\frac{(a-1)^{3/2}}{a}\left(\frac{\epsilon}{100}\right)\left(\frac{B_0}{B_{\rm Q}}\right)^{-1}\ {\rm erg\,cm^{-2}}. \quad (27)$$

Thus, the thickness of Eq.(25) and the surface tension of Eq.(27) for the DW indicate the dependence of $(T_{\rm d}-T)$, which is typical to the mean-field theory of continuous phase transitions. This is the reflection of the magnetic interactions leading the transition.

Furthermore, from Eqs.(25-27) we can quantify the thickness and surface tension with the outer crust structure and compositions for different magnetic fields in Tables 1-4. But we can get the qualitative properties of the thickness and tension by combining Eq.(14). In the deep outer crust with a fixed Fermi energy and $a \gg 1$, the thickness and tension are inversely proportional to B_0 and $B_0^{7/4}$, respectively. The result implies that a magnetar is relatively easy to experience depinning transitions than a normal neutron star because a magnetar is thinner and has a low tensional DW (which will be discussed in section 5.2).

The above calculations of the thickness and surface tension of DW do not involve the elastic energy of the crystal background given in Eqs.(23) and (24). These results underestimate the actual thickness and overestimate the surface tension. Probably, the cyclotron diameter plays the role of the lower limit of the DW thickness.

4.2. The Condon domain size

For the simplest domain structure with parallel and anti-parallel (along z direction) magnetizations, the sizes of the domain thickness (along x direction) δX and the domain (or DW) width δZ can be calculated approximately. The size of DW has been given in Eq.(25) or Eq.(26). In each layer of the transition where the magnetic field is assumed to be a constant, the Fermi energy increases with the depth below the surface of the neutron star. The variation of the Fermi energy corresponding to the phase difference 2π of the sinusoidal argument in Eq.(13) determines the thickness of domains and DWs. Provided that the surface gravity is supported by the degenerate electron pressure, the thickness is similar to the

result of Blandford & Hernquist (1982)

$$\delta Z \approx 50 g_{14}^{-1} Y_{\rm e} \left(\frac{\epsilon}{100}\right)^{-1} \frac{B_0}{B_{\rm Q}} \ {\rm cm}, \qquad (28)$$

where the surface gravity is $g = 10^{14} g_{14}$ cm s^{-2}. This result indicates the thickness of the domain and DW is proportional to the magnetic field at a fixed region. For a fixed magnetic field configuration the thickness is reverse proportional to the electron Fermi energy. At the deep outer crust of a magnetar with the Fermi energy 25 MeV and the magnetic field $10B_{\rm Q}$, the computed thickness is about 306 cm.

The reason of the existence of the Condon domain is that the magnetostatic energy is greatly reduced. This magnetostatic energy comes dominantly from the domains and the DWs. First we consider magnetostatic energy of the simplest domain structure in which there are many plate-like domains with a magnetization $M_{\rm s}$ along the $+z$ or $-z$. Bearing in mind that the domain thickness in the z-direction is larger than that in the x-direction, we can simplify the domains by extending indefinitely in the $-z$ direction. Using the method of magnetic potential which is induced by the magnetic free poles at the surface of the transition layer, the magnetostatic energy can be calculated. This calculation was carried out by Kittel (1949) and the magnetostatic energy per unit area of the surface $\varepsilon_{\rm m}$ is $\varepsilon_{\rm m} = 0.85 M_{\rm S}^2 \delta X$. In fact, on the top and bottom of the surface there exits same free poles with opposite signs, so that the magnetostatic energy is given by two times of the result. On the other hand, the total area of DWs per unit area of the surface is $\delta Z/\delta X$. The equilibrium domain thickness is given by minimizing the total energy, $\varepsilon_{\rm m} = 1.7 M_{\rm S}^2 \delta X + \sigma \delta Z/\delta X$. Solving $\frac{d\varepsilon_{\rm m}}{d\delta X} = 0$, we have the size of the domain thickness, $\delta X = 0.77\sqrt{\sigma \delta Z}/M_{\rm S}$, which is in the same way to be proportional to the geometric average of the domain width and the DW thickness as in ferromagnetic materials in spite of different phase transition mechanisms. Combining Eqs.(22),(27) and (28), the size is

$$\begin{aligned} \delta X &= 4.2 \times 10^2 Y_{\rm e}^{1/2} g_{14}^{1/2} (a-1)^{1/4} \left(\frac{\epsilon}{100}\right)^{3/2} \\ &\quad \times \left(\frac{B_0}{B_{\rm Q}}\right)^{-3/2} {\rm cm}. \end{aligned} \qquad (29)$$

At the deep outer crust of the magnetar with the Fermi energy 25 MeV and the magnetic field $10B_{\rm Q}$, the computed domain size along the x direction is about 4.4 cm, which is actually less than the domain thickness of 306 cm.

All of these results indicate that the outer crust of a neutron star consists of discrete Condon domain laminas whenever the diamagnetic phase of the electron gas occurs. The size of each domain lamina is given roughly by Eqs.(28) and (29).

5. Possible observational effects in magnetars

With the natural presences of a very large Fermi energy, strong or super-strong magnetic field, relatively low temperature and Dingle temperature, the diamagnetic phase can occur unprecedentedly inside the outer crust of a neutron star. Available magnetic free energy increases rapidly as B_0^4 because of the nonlinear magnetization. Except the discrepancy of the interaction mechanism, the diamagnetic phase is qualitatively the same as the ferromagnetic phase. Many observational effects in ferromagnetic materials such as magnetostriction, magnetocaloric (Gschneidner et al. 2005) and Barkhausen effects etc., should have their counterparts in a neutron star. Especially, the crust fracture due to the sharp magnetostriction or the intermittent motion of DWs can release elastic energy and the magnetic free energy deposited in the outer crust. This released energy can provide (or partially) the observable emissions from magnetar.

5.1. Magnetostriction effects

Accompanying the Landau quantization, all kinds of thermodynamic quantities such as the thermodynamic potential density of Eq.(23) and its derivative, the temperature and specific heat, the electron Fermi energy etc., oscillate depending on the field variation. This variation of the Fermi energy results from the oscillatory field dependence of the volume of the electron gas under a fixed pressure. In general the formation or adjustment of domain structure involves anisotropic magnetostrictive stress. The magnetostriction will be balanced by elastic stress in the lattice of the solid crust, provided that it was beyond the yield stress. Having considered the additional contribution of lattice stress energy to the thermodynamic

potential density of the outer crust system, the lattice strain can be determined by its derivative with respect to the stress. If explicitly taking the elastic energy into account, the generalized thermodynamic potential density Ω' of Eq.(23) can be expressed in terms of the stress tensor σ in the form,

$$\Omega' = \Omega - \frac{1}{2}(S_{ikpq})_0 \sigma_{ik}\sigma_{pq}. \quad (30)$$

In the absence of the magnetic field, here the elastic compliance tensor is denoted by $(S_{ikpq})_0$. Therefore, the second term on the right-hand side of Eq.(30) is only the elastic energy of the lattice stressed by the external stress. Due to electrical neutrality, the deformation of electron gas is identical with the lattice strain. The first term on the right hand of Eq.(30) includes the thermodynamic potential density of electron gas, in which the Fermi energy (or the oscillatory frequency) can change as changing the field. Corresponding to a given stress σ_{ik}, the strain is, $\varepsilon_{ik} = -\partial\Omega'/\partial\sigma_{ik} = \widetilde{\varepsilon}_{ik} + (S_{ikpq})_0\sigma_{pq}$. Here, we are only interested in the term of oscillatory magnetostriction, $\widetilde{\varepsilon}_{ik} = -\partial\Omega/\partial\sigma_{ik}$, which is given approximately by $\widetilde{\varepsilon}_{ik} = -(\partial \ln F/\partial\sigma_{ik})MB_0$. A more detailed discussion about this result can be found in Shoenberg (1984). For a spherical Fermi surface of free electrons, its volume is inversely proportional to the gas volume V as varying the stress. For this simplification and the linear relation of F to the area A (see Eq.(3)), we have $\partial \ln F/\partial\sigma_{ik} = -\frac{2}{3}(\partial \ln V/\partial\sigma_{ik})$. If neglecting the anisotropy of the compressibility coefficient and the Poisson ratio, we obtain $\partial \ln F/\partial\sigma_{ik} = -G/3$, where G is the shear modulus.

In the deep crust of a neutron star, the lattice rigid with respect to the terrestrial standard is enormous with a shear modulus about 2×10^{29} dyn cm^{-2} (Ruderman 1991) in most of the crust region of interest. For the magnetization $\pm M_{\rm S}$ of Eq.(22), the strain resulting from the domain formation is

$$\widetilde{\varepsilon} = \pm 2 \times 10^{-7}(1 - \frac{1}{a})^{1/2}(\frac{\epsilon}{100})^{-2} \times \left(\frac{G}{2 \times 10^{29}}\right)^{-1}\left(\frac{B_0}{B_{\rm Q}}\right)^3. \quad (31)$$

The result of Eq.(31) shows that the magnetostrictive stain is proportional to the third power of the central magnetic field in a cycle if a can be approximately treated as a constant and the crust can bear before yielding. In spite of unknowing quantitatively the limiting strain, the order of magnitude estimate of $\widetilde{\varepsilon}_{\rm m}$ in the deep crust (Smoluchowski & Welch 1970) is, $\widetilde{\varepsilon}_{\rm m} \sim 10^{-5} - 10^{-3}$. The strain of Eq.(31), for a normal neutron star with a magnetic field $B_* = 0.1$ and $\psi_0 = 25$ MeV in Table-4, is only about 8.0×10^{-10}. The normal neutron star can not be cracked by the magnetostriction. The least magnetic field required for cracking the deep outer crust is about (2.3-10.8)$\times B_{\rm Q}$.

The magnetar magnetic field of $B_0 \sim 10^{14} - 10^{15}$G (Woods & Thompson 2006) inferred from the observational spin down of magnetic braking is enough to crack the crust according to the magnetostriction model. Illustrated as by the same case of a normal neutron star above but with the magnetic field of a magnetar, $B_* = 10$, the strain is about 7.6×10^{-4} in the range of the limiting strain of $10^{-5} - 10^{-3}$. This rupture will suddenly release both of the magnetic and crustal elastic energies in the form of the Alfven waves. Duncan and Thompson (Duncan & Thompson 1992; Thompson & Duncan 1995b) had supposed that neutron stars with fields beyond the quantum magnetic field of $B_{\rm Q}$ are the sources of SGRs and AXPs bursts. Their proposed trigger mechanism of bursts is also the solid crust fracture, but the origin is the diffusing crustal magnetic field when built up sufficiently the Maxwell stress. In fact, the sharply magnetizing of the electron gas is an important or dominant contribution to the crustal fracture or plastic flow. If the bursts energy derives truly from this part of the free magnetic energy, the available maximum energy can be approximated to (detailed computation see Wang et al. (2013)), $E_{\rm m} = \frac{8\pi^2}{3}M_{\rm S}^2R_*^3$, with the neutron star radius R_*. The maximum energy is the order of magnitude $10^{38}(\frac{B_0}{B_{\rm Q}})^4$ erg as scaling R_* to 10 km, ϵ to 100 and a to ∞. Comparing the typical repeat burst energy $E_{burst} < 10^{41}$ ergs with the estimated energy, the result indicates that the sudden crustal fracture and the displacement of the magnetic footpoints driven by the magnetostriction release enough energy to power the SGRs and the AXPs repeat events. If the inferred dipolar magnetic field 7.5×10^{12} G of SGR 0418+5729 (Rea et al. 2010) is the lowest magnetic field magnetar, the least energy available

for observations is only about 10^{34} ergs. Such a low magnetic field does not crack the neutron star crust. We need new burst models to explain the low magnetic field magnetar (like-magnetar) emission.

5.2. Barkhausen effects

In Eq.(24), except ignoring the elastic energy of the solid crust we do not consider the crystal disorders and defects as well. However, once these are taken into account, an additional term should appear in the right-hand side of the equation which is called quenched noise. This general equation describing the motion of a driven interface in disordered medium belongs to the KPZ equation (Kardar et al. 1986). Arising from the quenched randomness, a pinned phase of the driven interface can exist under the absence of an external field or it is lower than a threshold value (determined by the disordering). As increasing the driving field, the interface motion must experience a phase transition from the pinned phase to a slowly smooth motion phase interspersed with jumps. This is an example of the so-called depinning phase transition.

The intermittent motion of DW in ferromagnetic materials (i.e., the BK effect) has been studied extendedly by both experimental and theoretical methods. All the essential elements of the BK effect as discovered by experiments are the statistical properties of the magnetization noise: distributions of duration and sizes of the avalanches, etc. The BK noise is self-similar, and shows scaling invariance or the power law distribution of statistical measure. In other words, it has the typical features of a self-organized criticality (Aschwanden et al. 2014). The exponent of the avalanche size scales as a function of the constant change rate C of the external field, and fluctuation D of the effective pinning field with Brownian correlations (Zapperi et al. 1998). The result of Zapperi et al. (1998) is

$$\tau = 3/2 - C/2D \ . \tag{32}$$

Behaving like all the first-order transitions, we expect that the motion of DWs in the diamagnetic phase is similar to the Barkhausen effect. It is natural to expect all the phenomena respecting to such a diamagnetic phase, e.g., nucleation, hysteresis and supercooling. The first hysteresis in the dHvA effect during the Condon domain formation has been discovered in beryllium (Kramer et al. 2005). Actually, the hysteresis is very small because of a high quality single crystals demand and (or) perhaps the large thickness of DW (Egorov 2010). Such a very small Dingle temperature and a relatively large rate of the field can prevent DW pinning at lattice point defects during wall movement in this experiment. However, the situations of a neutron star with a very lowly magnetic field evolution and high crystal disorder are significantly different from the hysteresis test in beryllium.

If treating the interface of the domains of a neutron star as an infinite-range elastic membrane with a fixed surface energy, and simplifying the disordering as pointlike defects with Brownian correlations we can expect the intermittent motion of DW with a power-law avalanche size distribution. Supposing that the bursts of SGR 1806-20 originate indeed from the depinning transition, the observable power law index $\tau \approx 1.6$ (Cheng et al. 1996) indicates that the constant C/D of Eq.(32) is about -0.2. The minus sign means the decay of the magnetic field. The non-small amplitude implies that the long-range correlation of the effective pinning field is not due to the internal correlation of the impurities. Actually, these impurities are either uncorrelated or only short-range correlated. The real disorders determine the Ohmic decay with a timescale larger than the Hall timescale at late times of a neutron star. In this regime, the Hall effect dominates the evolution of the crustal currents with a timescale depending strongly on the internal field. For a typical crust of $Y_{\rm e} = 0.25$, $g_{14} = 1$, the Hall timescale (Cumming et al. 2004) has an approximate value, $\tau_{\rm H} \sim 5.7 \times 10^4 \rho_{12}^{5/3}/B_{12}$ yrs ($B_{12} = B_0/10^{12}$). According to the timescale, $\tau_{\rm H}$, and the fundamental frequency, b, appearing in Eq.(13), a cycle of the dHvA magnetic oscillation actually corresponds to a temporal period, $T_{\rm osci} \sim 0.25\rho_{12}$ yrs. During this period, only a piece of the time associates with the formation of the diamagnetic phase. In the outer crust, we can expect that the jerky motion occurs frequently because of the short cycle period and the many layers of the dHvA oscillations. The outbursting emission observed in transient magnetars may be ascribed to the continually occurring of many depinning transitions. In the deep crust, however,

not only the burst active seldom is stronger than in that the outer crust, but also the BK noise. If we take $\rho_{12} = 6$, the electron gas dominates the pressure, an expected burst active period of 1.5 yrs between successive actives is roughly in agreement with the observation of 2.4 yrs in SGR 1806-20 (Laros et al. 1987).

However, as in the usual first-order phase transition, if there is not sufficient nucleation there may be a delay analogous to supercooling. Deep in the Fermi liquid of the nucleus of a neutron star, the domain structure does not appear because of the absence of the disorders. Instead of the formation of the Condon domain, there will be a metastable state corresponding to a homogeneous magnetization. As the magnetized system evolves into the spinodals of both homogeneous and coexisting phases or undergoes a large perturbation of the crust quake or BK noise, the loss balance of the metastable state would accompany sharply variations of the internal field which perhaps associates with the mechanism of giant flares (energies in range $10^{44} - 10^{46}$ ergs) (Mazets et al. 1979; Hurley et al. 1999; Palmer et al. 2005).

6. Conclusions

We have applied the Lifshitz-Kosevich-Shoenberg formula to dense matter with a relativistic electron gas. For a large Fermi energy (having a large Landau quantum number), the oscillatory properties of both no-relativistic and relativistic gases have the same form after the simple replacement of the cyclotron mass by the relativistic mass. Moreover, comparing with the no-relativistic gas, the magnetic interaction of electrons of a neutron star is strong enough to cause the diamagnetic phase transition. At the low magnetic field end of the phase transition curve, the phase-transition and the Dingle temperatures are determined simply by the existence of the dHvA oscillation, i.e., $\hbar\omega_{\rm c} \geq kT$ and $\hbar\omega_{\rm c} \geq kT_{\rm D}$. Except the distinction of interaction mechanisms, the diamagnetic phase transition is similar to the ferromagnetic phase transition. By the same considerations as in ferromagnetic materials, the special Condon domain configuration, its size, and the surface tension of DW in a neutron star have been calculated approximately.

In the observation of a neutron star, we suggested the connection between the magnetar emission and the magnetostriction or the Barkhausen effect. Due to the additional anisotropic stresses associated with the diamagnetic phase, the solid crust of a magnetar can be fractured which can trigger the observable X- or $\gamma-$ ray bursts. This is consistent with the radiation mechanism of the Duncan and Thompson model. However, another self-organized criticality of the BK effect can also explain the magnetar bursts. Here, the driver of the self-organized system is the slowly and continuously diffusive internal magnetic field due to the Hall effect and the ohmic decay. The instability threshold is the pinning threshold which does not reflect peculiar long-range correlations of the disorders, but indicates an effective description of the collective motion of the interface (Cizeau et al. 1997). Emergence of the magnetic flux by magnetizing builds up the non-potential free magnetic energy that can be released in the subsequent avalanches. This process of energy releasing may be very efficient because of the damping of the long-range correlatively effective pinning field acting on the Hall drift. The mechanism makes the Hall effect itself become dissipative but be distinct from the Hall cascade. With the new energy releasing mechanism, we can explain the low-field magnetar bursts, the heating mechanism of transient magnears, and the trigger mechanism of giant flares, etc. However, more observational evidences and theoretical comparisons are needed to test the new mechanism.

ACKNOWLEDGMENTS

We thank the anonymous referee for his/ her comments which helped to improve the paper. ZJ thanks Prof. Anzhong Wang for correcting the English language of the manuscript.This work was supported by XinJiang Science Fund for Distinguished Young Scholars under Nos. 2014721015 and 2013721014, the National Science Foundation of China (Grants Nos. 11503008, 11473024, 11363005, 11163005 and 11264037), and the Doctor Foundation of Xinjiang University (Grant No.BS110108).

REFERENCES

Alessandro, B., Beatrice, C., Bertotti, G., & Montorsi, A. 1990, Journal of Applied Physics, 68,

2908

Aschwanden, M. J., et al. 2014, Space Science Reviews

Bakaleinikov, L. A., & Gordon, A. 2012, Physica B Condensed Matter, 407, 3408

Basilico, D., Arteaga, D. P., Roca-Maza, X., & Colò, G. 2015, Phys. Rev. C, 92, 035802

Blandford, R. D., & Hernquist, L. 1982, Journal of Physics C Solid State Physics, 15, 6233

Chamel, N., et al. 2012, Phys. Rev. C, 86, 055804

Chen, K., Bak, P., & Obukhov, S. P. 1991, Physical Review A, 43, 625

Cheng, B., Epstein, R. I., Guyer, R. A., & Young, A. C. 1996, Nature, 382, 518

Cizeau, P., Zapperi, S., Durin, G., & Stanley, H. E. 1997, Physical Review Letters, 79, 4669

Coldwell-Horsfall, R. A., & Maradudin, A. A. 1960, Journal of Mathematical Physics, 1, 395

Condon, J. H. 1966, Physical Review, 145, 526

Cumming, A., Arras, P., & Zweibel, E. 2004, Astrophys. J., 609, 999

Duncan, R. C., & Thompson, C. 1992, ApJ, 392, L9

Durin, G., & Zapperi, S. 2004, eprint arXiv:cond-mat/0404512

Egorov, V. S. 2010, Physics Uspekhi, 53, 755

Engelsberg, S., & Simpson, G. 1970, Phys. Rev. B, 2, 1657

Goldreich, P., & Reisenegger, A. 1992, ApJ, 395, 250

Gordon, A., Itskovsky, M. A., & Wyder, P. 1999, Phys. Rev. B, 59, 10864

Gordon, A., Vagner, I. D., & Wyder, P. 2003, Advances in Physics, 52, 385

Goriely, S., Chamel, N., & Pearson, J. M. 2010, Phys. Rev. C, 82, 035804

GöğüŞ , E., Woods, P. M., Kouveliotou, C., van Paradijs, J., Briggs, M. S., Duncan, R. C., & Thompson, C. 1999, Astrophys. J., 526, L93

Gschneidner, Jr., K. A., Pecharsky, V. K., & Tsokol, A. O. 2005, Reports on Progress in Physics, 68, 1479

Horowitz, C. J., & Kadau, K. 2009, Physical Review Letters, 102, 191102

Hurley, K., et al. 1999, Nature, 397, 41

Ibrahim, A. I., et al. 2004, Astrophys. J., 609, L21

Ingraham, R. L., & Wilkes, J. M. 1987, Ap&SS, 135, 87

Itoh, N., & Kohyama, Y. 1993, ApJ, 404, 268

Johnson, M. H., & Lippmann, B. A. 1949, Physical Review, 76, 828

Jones, P. B. 2001, MNRAS, 321, 167

Kardar, M., Parisi, G., & Zhang, Y.-C. 1986, Physical Review Letters, 56, 889

Kittel, C. 1949, Reviews of Modern Physics, 21, 541

Kramer, R. B. G., Egorov, V. S., Gasparov, V. A., Jansen, A. G. M., & Joss, W. 2005, Physical Review Letters, 95, 267209

Lai, D., & Shapiro, S. L. 1991, ApJ, 383, 745

Landau, L. D., & Lifshitz, E. M. 1969, Statistical physics. Pt.1, ed. Landau, L. D. & Lifshitz, E. M.

Laros, J. G., et al. 1987, Astrophysics Journal Letters, 320, L111

Li, X. H., Gao, Z. F., Li, X. D., Xu, Y., Wang, P., Wang, N., & Peng, Q. H. 2016, International Journal of Modern Physics D, 25, 1650002

Lifshits, E. M., & Kosevich, A. M. 1956, Zh. Eksp. Teor. Fiz., 29, 730

Lu, E. T., Hamilton, R. J., McTiernan, J. M., & Bromund, K. R. 1993, Astrophys. J., 412, 841

Luttinger, J. M. 1960, Physical Review, 119, 1153

Mazets, E. P., Golentskii, S. V., Ilinskii, V. N., Aptekar, R. L., & Guryan, I. A. 1979, Nature, 282, 587

Mereghetti, S. 2008, The Astronomy and Astrophysics Review, 15, 225

Narayan, O. 1996, Physical Review Letters, 77, 3855

Palmer, D. M. 1999, Astrophysics Journal Letters, 512, L113

Palmer, D. M., et al. 2005, Nature, 434, 1107

Pons, J. A., Link, B., Miralles, J. A., & Geppert, U. 2007, Physical Review Letters, 98, 071101

Pons, J. A., & Rea, N. 2012, Astrophys. J., 750, L6

Privorotskii, I. A. 1976, Thermodynamic Theory of Domain Structures, ed. Landau, L. D. & Lifshits, E. M.

Rea, N., et al. 2010, Science, 330, 944

Ruderman, R. 1991, Astrophys. J., 382, 576

Shoenberg, D. 1962, Royal Society of London Philosophical Transactions Series A, 255, 85

—. 1984, Magnetic oscillation in metals, 32–66

Smoluchowski, R., & Welch, D. O. 1970, Physical Review Letters, 24, 1191

Solt, G., Baines, C., Egorov, V. S., Herlach, D., Krasnoperov, E., & Zimmermann, U. 1996, Physical Review Letters, 76, 2575

Solt, G., Baines, C., Egorov, V. S., Herlach, D., & Zimmermann, U. 1999, Phys. Rev. B, 59, 6834

Solt, G., & Egorov, V. S. 2002, Physica B Condensed Matter, 318, 231

Solt, G., Egorov, V. S., Baines, C., Herlach, D., & Zimmermann, U. 2000, Phys. Rev. B, 62, 11933

Suh, I.-S., & Mathews, G. J. 2010, Astrophys. J., 717, 843

Thompson, C., & Duncan, R. C. 1995a, MNRAS, 275, 255

—. 1995b, Monthly Notices of the Royal Astronomical Society, 275, 255

Turolla, R., Zane, S., & Watts, A. 2015, ArXiv e-prints

Wang, Z., Lü, G., & Zhu, C. 2014, Astrophysics and Space Science, 353, 651

Wang, Z., Lü, G., Zhu, C., & Huo, W. 2013, ApJ, 773, 160

Woods, P. M., & Thompson, C. 2006, Soft gamma repeaters and anomalous X-ray pulsars: magnetar candidates, ed. W. H. G. Lewin & M. van der Klis, 547–586

Zapperi, S., Cizeau, P., Durin, G., & Stanley, H. E. 1998, Phys. Rev. B, 58, 6353

This 2-column preprint was prepared with the AAS LaTeX macros v5.2.